

Walking Primitive Synthesis for an Anthropomorphic Biped using Optimal Control Techniques

J Denk and G Schmidt

Institute of Automatic Control Engineering, Technische Universität München, D-80290 Munich, Germany

ABSTRACT

This paper presents a mathematical method for generating walking primitives for an anthropomorphic 3D-biped with 12 joints. The corresponding rigid body model includes all masses and inertia tensors. Control torques allowing a symmetrical straight ahead gait with pre-swing, swing and heel-contact are derived by dynamic optimization using a direct collocation approach. The computed torques minimize the absolute value of the mechanical power consumption in the joints of the biped. Zero moment point (ZMP) and friction conditions at the feet ensuring postural stability of the biped, as well as bounds on the joint angles and on the control torques, are treated as constraints. The resulting biped motion is dynamically stable and the overall motion behaviour is remarkably close to that of humans.

1 INTRODUCTION

Autonomous walking requires the ability of a biped to adapt its gait pattern according to the present environmental situation, so that obstacles in the walking trail can be passed by or overcome. One method for achieving this capability is to compute a set of stable walking primitives for steps with different parameters offline and to store them in a database. A situation-dependent walking pattern can then be obtained by selection and concatenation of appropriate walking primitives during run-time [8]. Often, the problem of walking primitive synthesis is simplified by prescribing time trajectories for selected body parts [9, 10, 12]. The task of determining suitable trajectories thereby strongly depends on the designer's intuition and/or observations and biometric measurements of human gait behaviour.

In this paper a method for synthesizing dynamically stable walking primitives [10] with three gait phases, namely pre-swing, swing and heel-contact, is described. In contrast to the methods mentioned earlier only step-length, step-width and the temporal succession of the gait phases are used to specify the desired motion. The walking primitive then results as the solution of a multi-phase optimal control problem minimizing the absolute mechanical power consumption in the biped's joints. Zero moment point (ZMP) and friction conditions, as well as bounds on the joint angles and on the control torques, are considered as constraints and ensure the feasibility of the trajectory. The optimal control problem is solved numerically by discretization of time

using a direct-collocation approach [11]. The method of direct-collocation has already been applied successfully to synthesize a walking primitive for a planar biped [6]. Other examples for energy optimal planar walking can be found in [1, 2].

2 WALKING MACHINE

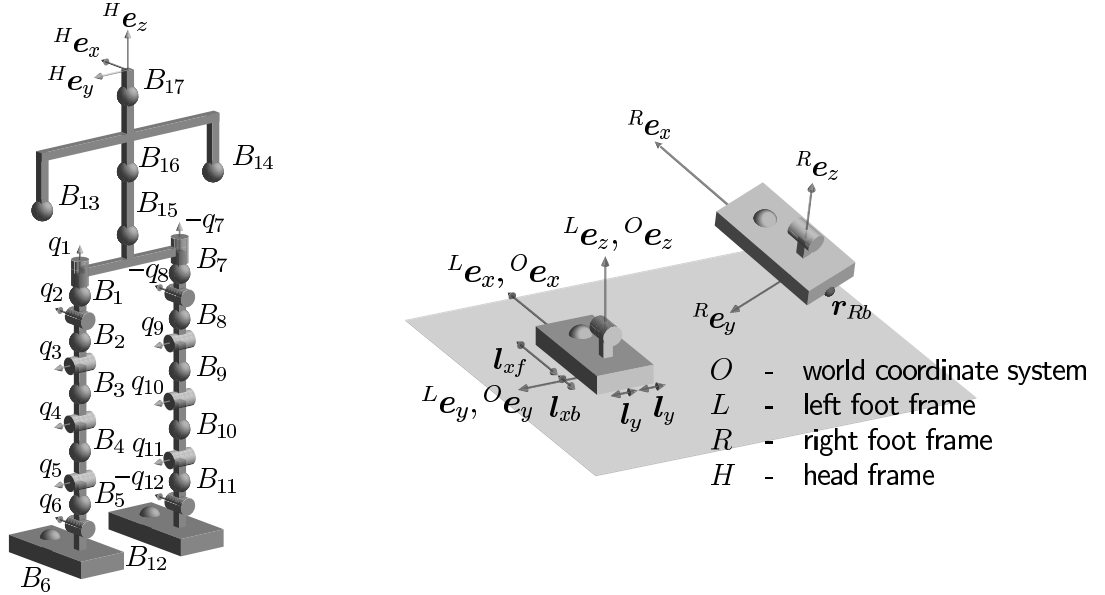


Fig. 1. Kinematic scheme of the biped robot (left) and feet with coordinate-systems (right).

The walking machine considered here is illustrated in Figure 1. It is based on a simplified model of the biped robot “Johnnie” [4] developed at the TU-München. The model comprises 17 bodies $B_1 \dots B_{17}$ together with their complete inertia characteristics. Three joints are located in each hip, one joint in the knees and two joints in the ankles resulting in the vector of joint angles $\mathbf{q} = [q_1 \dots q_{12}]^T$. Four coordinate systems are defined, the world frame O , the head frame H and the contact frames L and R fixed in the sole of the left and right foot respectively. The pose of H , L and R with respect to O is given by $\mathbf{p}_H = [\mathbf{r}_H, \boldsymbol{\phi}_H]$, $\mathbf{p}_L = [\mathbf{r}_L, \boldsymbol{\phi}_L]$ and $\mathbf{p}_R = [\mathbf{r}_R, \boldsymbol{\phi}_R]$. The elements of vector $\mathbf{r} = [r_x \ r_y \ r_z]^T$ are Cartesian coordinates, $\boldsymbol{\phi} = [\phi_x \ \phi_y \ \phi_z]^T$ are orientations represented by roll-, pitch- and yaw-angles. The posture of the biped is defined by the generalized coordinates $\mathbf{q}_g = [\mathbf{q}, \mathbf{p}_L]$.

3 WALKING PRIMITIVE SPECIFICATION

As already mentioned in the introduction, the regarded walking primitive comprises the 3 phases *pre-swing*, *swing* and *heel-contact* and represents a single step in the sagittal plane with the right foot swinging, see Figure 2. The left foot resides flat on the ground in the origin of the world coordinate system O given by $\mathbf{p}_L(t) = \mathbf{0}, \forall t \in [0, t_s]$. With the transformation

$$\mathbf{q}_g(t) = \begin{bmatrix} \mathbf{q}(t) \\ \mathbf{p}_L(t) \end{bmatrix} = \begin{bmatrix} \mathbf{E} \\ \mathbf{0} \end{bmatrix} \mathbf{q}(t), \forall t \in [0, t_s],$$

where E is the unity matrix, the system can then be described in minimal coordinates $\mathbf{q}(t)$ for this contact situation reducing the number of system states during walking primitive synthesis from 2×18 to 2×12 .

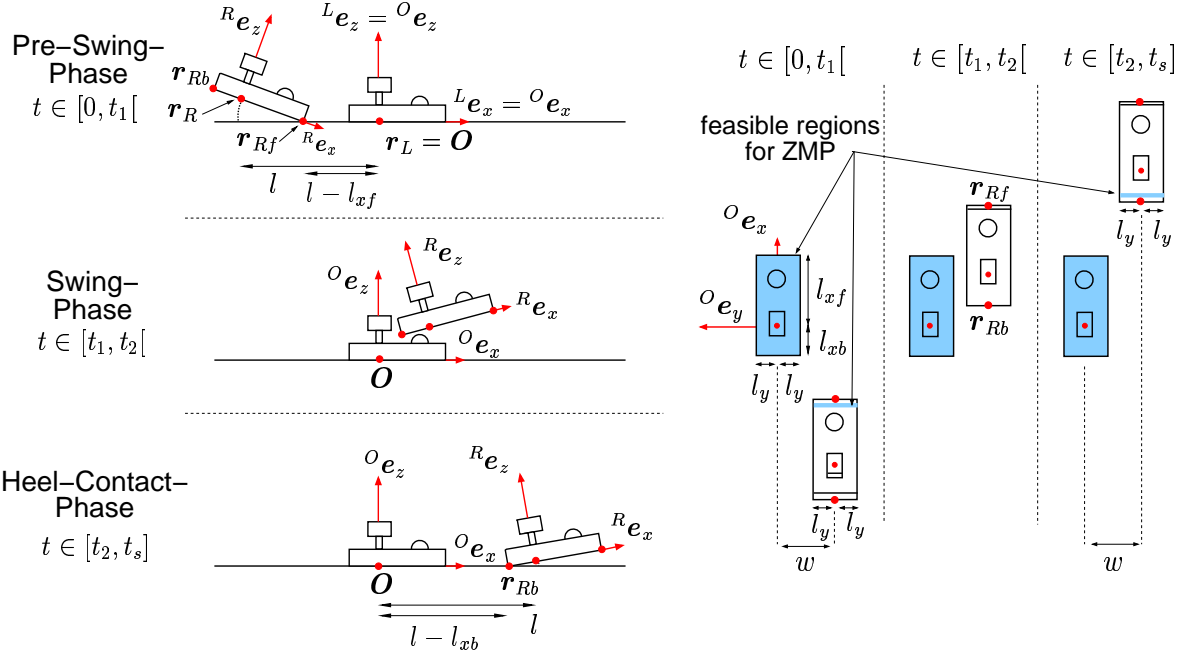


Fig. 2. Three phases of a walking primitive, side and top view. Feasible regions for ZMP.

In order to avoid undesirable mechanical stress, the trajectory $\mathbf{q}(t)$ is constrained to be continuous and continuously differentiable with respect to time. This implies that there are no jumps in the Cartesian velocities of the right foot and thus no impacts when the heel contacts the ground.

During swing-phase the mechanism of the biped forms an open kinematic chain. During pre-swing and heel-contact, however, both feet contact the ground and a closed loop forms. This is taken into account by kinematic constraints imposed on the system accelerations. These constraints and all other boundary conditions and inequality constraints necessary to characterize the kinematics of the walking primitive for the optimization process are summarized in the following. The relevant parameters step length l , step width w , phase-transition-times t_1 and t_2 and step-duration t_s are provided as input to the optimization problem.

- **Start of the Walking Primitive:** $t = 0$: The right foot is located flat on the ground. Pose and velocity are given by the boundary conditions

$$\mathbf{p}_R(0) = [-l \ -w \ 0 \ | \ 0 \ 0 \ 0]^T \quad \text{and} \quad \begin{bmatrix} {}_O\dot{\mathbf{r}}_R(0) \\ {}_O\boldsymbol{\omega}_R(0) \end{bmatrix} = \mathbf{C}_R(\mathbf{q}(0)) \dot{\mathbf{q}}(0) = \mathbf{0}, \quad (1)$$

where \mathbf{C}_R is a Jacobian matrix, ${}_O\dot{\mathbf{r}}_R$ and ${}_O\boldsymbol{\omega}_R$ are the Cartesian and angular velocities represented in the world frame O . The respective initial joint angles and joint velocities are denoted $[\mathbf{q}_0, \dot{\mathbf{q}}_0] = [\mathbf{q}(0), \dot{\mathbf{q}}(0)]$.

- **Pre-Swing-Phase:** $t \in]0, t_1[$: The right foot rolls over the toes. This contact situation is expressed by the kinematic constraint

$$\begin{bmatrix} {}_O\ddot{\mathbf{r}}_{Rf}(t) \\ {}_O\dot{\omega}_{R,x}(t) \\ {}_O\dot{\omega}_{R,z}(t) \end{bmatrix} = \mathbf{C}_{Rf}(\mathbf{q}(t))\ddot{\mathbf{q}}(t) + \dot{\mathbf{C}}_{Rf}(\mathbf{q}(t))\dot{\mathbf{q}}(t) = \mathbf{0}, \quad \forall t \in]0, t_1[. \quad (2)$$

The heel stays above the ground which is ensured by the inequality constraint $r_{Rb,z}(t) \geq 0$.

- **Swing-Phase:** $t \in [t_1, t_2[$: The swing-phase starts with the right foot just about to leave the ground at $t = t_1$ and then swinging towards its new position. External collisions with the ground

and internal collisions with the left leg are avoided by the inequality constraints $r_{Rf,z}(t) \geq 0$, $r_{Rb,z}(t) \geq 0$, and $r_{Rb,y}(t) \leq -w_{min}$, with w_{min} representing a minimal distance between the left and right leg.

• **Heel-Contact-Phase:** $t \in [t_2, t_s[$: At $t = t_2$ the foot touches the ground and rolls around the heel. The corresponding kinematic constraint is given by

$$\begin{bmatrix} {}_O\ddot{\mathbf{r}}_{Rb}(t) \\ {}_O\dot{\omega}_{R,x}(t) \\ {}_O\dot{\omega}_{R,z}(t) \end{bmatrix} = \mathbf{C}_{Rb}(\mathbf{q}(t))\ddot{\mathbf{q}}(t) + \dot{\mathbf{C}}_{Rb}(\mathbf{q}(t))\dot{\mathbf{q}}(t) = \mathbf{0}, \quad \forall t \in [t_2, t_s[. \quad (3)$$

The toes have to remain above the ground which is ensured by $r_{Rf,z}(t) \geq 0$.

• **End of the Walking Primitive:** $t = t_s$: The right foot is flat on the ground again, pose and velocity are given by the boundary conditions

$$\mathbf{p}_R(t_s) = [l - w \ 0 \ | \ 0 \ 0 \ 0]^T \quad \text{and} \quad \begin{bmatrix} {}_O\dot{\mathbf{r}}_R(t_s) \\ {}_O\boldsymbol{\omega}_R(t_s) \end{bmatrix} = \mathbf{C}_R(\mathbf{q}(0)) \dot{\mathbf{q}}(0) = \mathbf{0}. \quad (4)$$

The respective final joint angles and velocities are denoted $[\mathbf{q}_s, \dot{\mathbf{q}}_s] = [\mathbf{q}(t_s), \dot{\mathbf{q}}(t_s)]$. Taking advantage of the symmetry in the kinematic structure of the biped a walking primitive $\tilde{\mathbf{q}}(t)$ for the right foot supporting the biped is easily obtained from $\mathbf{q}(t)$ by the mapping

$$\tilde{\mathbf{q}}(t) = \begin{bmatrix} \mathbf{0} & \mathbf{E} \\ \mathbf{E} & \mathbf{0} \end{bmatrix} \mathbf{q}(t) \quad t \in [0, t_s].$$

Stating the additional boundary conditions relating the initial and final system state

$$\mathbf{q}_s = \tilde{\mathbf{q}}_0 \quad \text{and} \quad \dot{\mathbf{q}}_s = \dot{\tilde{\mathbf{q}}}_0 \quad (5)$$

thus allows the concatenation of the primitives to a smooth walking pattern $\mathbf{q}, \tilde{\mathbf{q}}, \mathbf{q}, \tilde{\mathbf{q}}, \mathbf{q}, \dots$ for continuous symmetric cyclic walking, cf. [8].

4 DYNAMICS AND CONDITIONS FOR CONTACT STABILITY

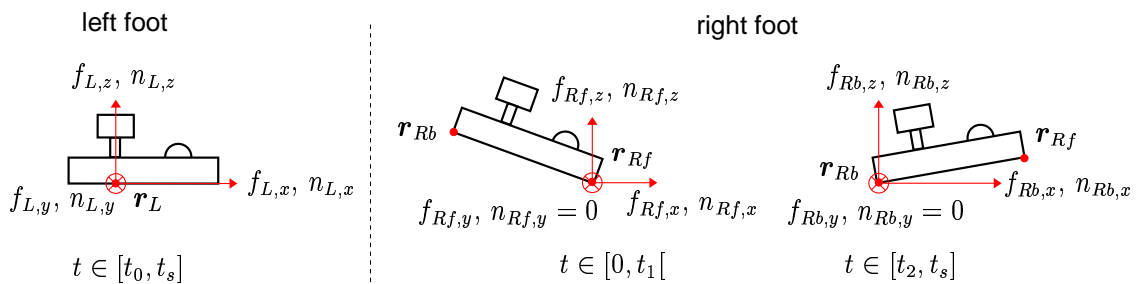


Fig. 3. Resultant contact forces and moments during each phase of the walking primitive.

The system dynamics in the three phases of the walking primitive are modeled under the assumption of bilateral rigid body contacts between the feet and the ground. The sum of all forces on a contact surface is thereby represented by the resultant contact forces $\mathbf{f} = [f_x \ f_y \ f_z]^T$ and moments $\mathbf{n} = [n_{Rf,x} \ n_{Rf,y} \ n_{Rf,z}]^T$ acting in the points $\mathbf{r}_L, \mathbf{r}_{Rf}, \mathbf{r}_{Rb}$ as shown in Figure 3 depending on the current walking phase.

The dynamics of the biped in minimal coordinates $\mathbf{q}(t) \in \mathbb{R}^{12}$ are then given by

$$\mathbf{M}(\mathbf{q})\ddot{\mathbf{q}} = \mathbf{h}(\mathbf{q}, \dot{\mathbf{q}}) + \boldsymbol{\tau} + \mathbf{C}_{Rf}(\mathbf{q})^T \mathbf{F}_{Rf} + \mathbf{C}_{Rb}(\mathbf{q})^T \mathbf{F}_{Rb} \quad (6)$$

with \mathbf{M} the mass-matrix, \mathbf{h} coriolis, centrifugal and gravity effects and $\boldsymbol{\tau}$ the joint torques. The Jacobian matrices $\mathbf{C}_{Rf} \in \mathbb{R}^{5 \times 12}$ and $\mathbf{C}_{Rb} \in \mathbb{R}^{5 \times 12}$ obtained in (2) and (3) are projecting the generalized constraint contact forces $\mathbf{F}_{Rb} = [\mathbf{f}_{Rb}, n_{Rb,x}, n_{Rb,z}] \in \mathbb{R}^{5 \times 1}$ and $\mathbf{F}_{Rf} = [\mathbf{f}_{Rf}, n_{Rf,x}, n_{Rf,z}] \in \mathbb{R}^{5 \times 1}$ on the generalized coordinates. As the contact situation of the left foot is formulated in minimal coordinates, the forces $\mathbf{F}_L = [\mathbf{f}_L, \mathbf{n}_L] \in \mathbb{R}^{6 \times 1}$ are not part of the dynamic system equations. However, they can be recalculated easily using the Principle of D'Alambert as soon as $\ddot{\mathbf{q}}$ and the external forces on the right foot have been determined, see also [10]. The system accelerations during *swing-phase* ($\mathbf{F}_{Rb} = \mathbf{F}_{Rf} = \mathbf{0}$) are computed as

$$\ddot{\mathbf{q}} = \mathbf{M}^{-1}(\mathbf{h} + \boldsymbol{\tau}) \quad , \quad \forall t \in [t_1, t_2[\quad . \quad (7)$$

During *pre-swing* ($\mathbf{F}_{Rb} = \mathbf{0}$) resp. *heel-contact* ($\mathbf{F}_{Rf} = \mathbf{0}$) the 5 additional equations (2) resp. (3) on the system accelerations are used to solve for $[\ddot{\mathbf{q}}, \mathbf{F}_{Rf}]$ resp. $[\ddot{\mathbf{q}}, \mathbf{F}_{Rb}]$ resulting in:

$$\begin{aligned} \ddot{\mathbf{q}} &= \mathbf{M}^{-1}(\mathbf{h} + \boldsymbol{\tau} + \mathbf{C}_{Rf/b}^T \mathbf{F}_{Rf/b}) \\ \mathbf{F}_{Rf/b} &= -(\mathbf{C}_{R/f} \mathbf{M}^{-1} \mathbf{C}_{Rf/b}^T)^{-1} (\mathbf{C}_{Rf/b} \mathbf{M}^{-1}(\mathbf{h} + \boldsymbol{\tau}) + \dot{\mathbf{C}}_{Rf/b} \dot{\mathbf{q}}) \quad , \quad \forall t \in [0, t_1[\quad / \quad [t_2, t_s] \quad . \end{aligned} \quad (8)$$

Up to this point, bilateral contacts have been assumed. In reality however, physical contacts are unilateral and contact stability conditions have to be considered as additional constraints ensuring that the resulting contact forces \mathbf{f} and \mathbf{n} are compatible with the present contact situation:

- **Unilaterality conditions** on the resultant normal contact forces ensure, that a desired contact situation does not change by a foot lifting off the ground:

$$f_{L,z} \geq 0, \quad \forall t \in [0, t_s] \quad ; \quad f_{Rf,z} \geq 0, \quad \forall t \in [0, t_1[\quad ; \quad f_{Rb,z} \geq 0, \quad \forall t \in [t_2, t_s] \quad . \quad (9)$$

- **ZMP conditions**, as introduced by Vukobratović [12], are used in this work to prevent a foot from beginning to rotate around its edges. The ZMP \mathbf{r}_p is defined as the point on the contact surface, where the resultant moments n_x, n_y of all contact forces are zero. If the ZMP remains inside the contact area the contact situation is stable.

With the resultant contact forces sketched in Figure 3 the ZMP \mathbf{r}_{pL} of the left foot, which should remain flat on the ground during all three phases, can be expressed in the left foot frame L as

$${}^L r_{pL,x} = -\frac{n_{Ly}}{f_{Lz}} \quad , \quad {}^L r_{pL,y} = \frac{n_{Lx}}{f_{Lz}} \quad .$$

The following constraints result from the area of valid ZMP positions illustrated in Figure 2 :

$$-l_{xb} \leq -\frac{n_{Ly}}{f_{Lz}} \leq l_{xf}, \quad -l_y \leq \frac{n_{Lx}}{f_{Lz}} \leq l_y, \quad \forall t \in [0, t_s] \quad . \quad (10)$$

As the right foot rotates around its front resp. back edge during pre-swing resp. heel-contact there is no resultant moment n_y and the contact surface degenerates to a line. The ZMP moves along this line while its coordinates in frame R are given by

$$\begin{aligned} {}^R r_{pR,y} &= \frac{n_{Rf,x}}{f_{Rf,z}}, \quad {}^R r_{pR,x} = l_{xf}, \quad \forall t \in [0, t_1[\\ {}^R r_{pR,y} &= \frac{n_{Rb,x}}{f_{Rb,z}}, \quad {}^R r_{pR,x} = l_{xb}, \quad \forall t \in [t_2, t_s] \quad . \end{aligned}$$

Considering the areas designated in Figure 2 now leads to the constraints

$$-l_y \leq \frac{n_{Rf,x}}{f_{Rf,z}} \leq l_y, \quad \forall t \in [0, t_1[; \quad -l_y \leq \frac{n_{Rb,x}}{f_{Rb,z}} \leq l_y, \quad \forall t \in [t_2, t_s] \quad (11)$$

which ensure that the front resp. back edge of the right foot remains flat on the ground.

• **Friction conditions** ensure that a supporting foot neither begins to slip on the ground nor starts to rotate around the normal axis e_z of the contact surface. Thereby resultant tangential forces f_x, f_y and resultant moments n_z cannot be treated independently, because their effects combine. Thus the friction condition [10]

$$\sqrt{f_x^2 + f_y^2} + \left| \frac{n_z}{\kappa} \right| \leq \mu f_z \quad (12)$$

is applied which has to be satisfied by the resultant contact forces \mathbf{F}_L of the left foot during all three phases, by \mathbf{F}_{Rf} at the right foot during pre-swing and \mathbf{F}_{Rb} during heel-contact. The first term in (12) is the usual friction cone, the second term an additional tangential force induced from the moment n_z . The constant $0 < \mu < 1$ denotes the friction coefficient of the rubbing surfaces and κ is the frictional radius. The frictional radius assumed is $\kappa_L = 0.5 \sqrt{(2l_y)^2 + (l_{xb} + l_{xf})^2}$ for the left foot and $\kappa_{Rf} = \kappa_{Rb} = l_y$ for the right foot during pre-swing and heel-contact.

5 FORMULATION OF THE OPTIMAL CONTROL PROBLEM

The instantaneous mechanical power P_i transmitted by a motor in the i -th joint of the biped is given as $P_i(t) = \dot{q}_i(t)\tau_i(t)$, with τ_i the motor torque. The energy released by the system when backdriving the motor ($P_i(t) < 0$) is usually not used for recharging the power source. This is regarded in the objective function by penalizing the sum of the absolute values of $P_i(t)$, $i = 1 \dots 12$, indicating, that power is actively consumed when dissipating this energy cf. [1].

The optimization problem formulated for calculating the joint torques required to drive the biped can then be summarized as follows:

$$\min_{\tau(t)} \left(\int_0^{t_1} \sum_{i=1}^{12} |\dot{q}_i(t)\tau_i(t)| dt + \int_{t_1}^{t_2} \sum_{i=1}^{12} |\dot{q}_i(t)\tau_i(t)| dt + \int_{t_2}^{t_s} \sum_{i=1}^{12} |\dot{q}_i(t)\tau_i(t)| dt \right) \quad (13)$$

with t_1, t_2 and t_s given and fixed, subject to:

(i) the differential equations (7), (8) of the system according to the actual motion phase; (ii) the contact stability conditions (9), (10), (11),(12); (iii) the inequality constraints for collision avoidance; (iv) phase connection conditions on the system state at $t = t_1$ and $t = t_2$ ensuring a steady state trajectory; (v) the boundary conditions (1) on the initial state and (5) allowing cyclic walking; (vi) continuous bounds on the joint-angles, joint-velocities and joint-torques in order to satisfy restrictions given by the mechanical and electrical design.

6 NUMERICAL RESULTS

Numerical results for a sample walking primitive are presented next. They were obtained by solving the optimal control problem stated in Section 5 with the direct-collocation software DIRCOL [11]. DIRCOL transcribes the continuous optimal control problem into a static optimization problem by discretization of trajectories in time. The resulting nonlinear programming

problem can then be solved with the sparse solver SNOPT [5]. All necessary dynamical equations were derived with the help of AUTOLEV [7], a tool for analytical motion analysis.

The following set of parameters was assumed: step-length $l = 0.35m$, step-width $w = 0.13m$, phase-transition-time $t_1 = 0.06s$, phase-transition-time $t_2 = 0.48s$, step-duration $t_s = 0.49s$ and friction coefficient $\mu = 0.7$. Although optimal control theory as well as DIRCOL allow for treating the temporal parameters t_1, t_2 and t_s as additional optimization variables they are treated here as fixed for purposes of improved convergence.

As a rough initial solution for the walking primitive a trajectory for statically stable walking, cf. [8], was chosen. Beginning with a coarse discretization a feasible solution could be generated, which was then used as a starting trajectory for subsequent optimizations. The computation time required strongly depends on the quality of the initial solution and on the fineness of the discretization. Using a current standard PC (Intel Pentium III 1.0 GHz) and 30 grid points the typical comparatively modest computation time is about two hours. The resulting trajectories for the position of the biped's center of mass (COM) in the world-coordinate system O and the orientation of the head frame given by RPY-angles ϕ_H are depicted in Figure 4. The Cartesian velocity in x -direction is almost constant. The relatively large oscillation in the pitch angle $\phi_{H,z}$ are due to a missing degree of freedom around the z -axis in the trunk of the biped and the fact, that the left foot resides flat on the ground. The motion of the head, center of mass and feet in the x - z -plane after concatenation of the walking primitive to a cyclic walking pattern are shown in the right side of Figure 4.

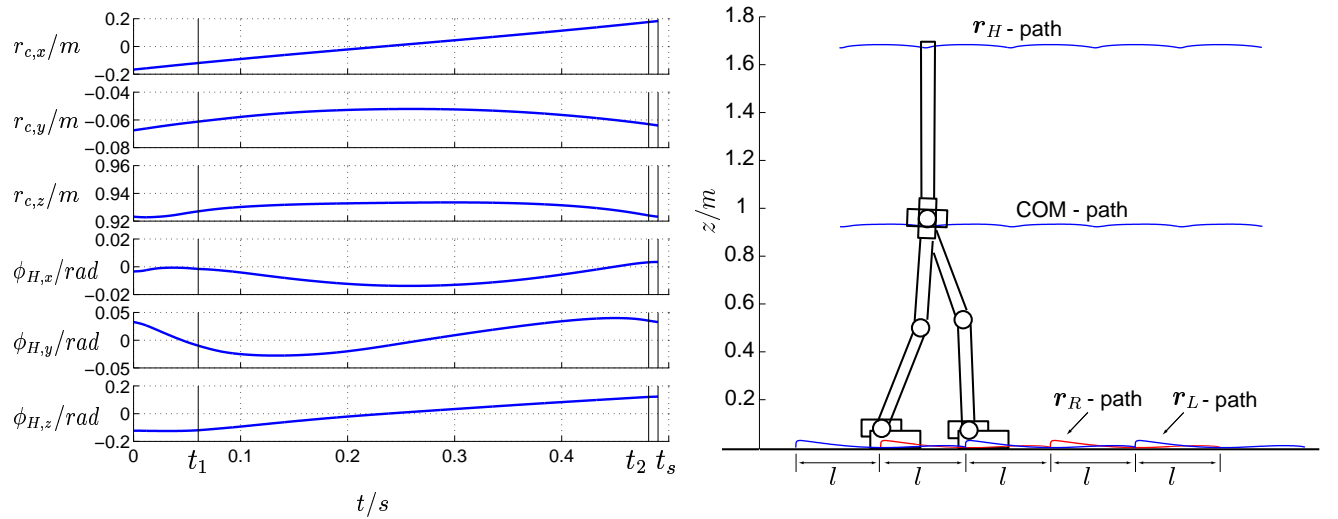


Fig. 4. Left: Resulting trajectories for position r_c of COM (center of mass) and orientation ϕ_H of biped head for sample walking primitive. Right: Path of head, COM and feet in the sagittal plane during cyclic walking with $l = 0.35m$.

7 CONCLUSIONS AND FUTURE WORK

The results presented demonstrate that dynamically stable, physically feasible and naturally looking walking primitives can be generated by optimal control techniques in reasonable time using direct collocation methods. Further investigations show that convergence improves significantly, when trajectories are searched in the vicinity of existing solutions. This fact and the strict mathematic nature of the approach seem to allow the automatic synthesis of a bigger set of

walking primitives with slightly varied parameters. In our future work we will make use of this property when we generate a database of primitives allowing walking with several step-lengths, as already presented in [8] for statically stable walking motion. In addition to straight ahead walking, curve walking and striding over obstacles will be considered. The resulting database will be used to provide the walking patterns required for perception-based goal-oriented walking of a biped robot [3].

ACKNOWLEDGMENTS

This work was supported in part by the German Research Foundation (DFG) within the “Autonomous Walking” Priority Research Program. We would also like to express our gratitude to O. von Stryk and P. E. Gill for making their programs DIRCOL and SNOPT available for this research.

REFERENCES

- [1] P.H. Channon, S.H. Hopkins, and D.T. Pham. Derivation of optimal walking motions for a bipedal walking robot. *Robotica*, 10:165–172, 1992.
- [2] S. Chesse and G. Bessonnet. Optimal dynamics of constrained multibody systems. Application to bipedal walking synthesis. In *Proc. of the IEEE Int. Conf. on Robot. and Autom.*, pages 2499–2505, Seoul, Korea, 2001.
- [3] J. F. Seara, G. Schmidt, and O. Lorch. ViGWaM Active Vision System— Gaze Control for Goal-Oriented Walking. In *Proc. of the Int. Conf. on Climbing and Walking Robots (CLAWAR)*, Karlsruhe, Germany, September 2001.
- [4] M. Gienger, K. Loeffler, and F. Pfeiffer. Towards the Design of a Biped Jogging Robot. In *Proc. of the IEEE Int. Conf. on Robot. and Autom.*, pages 4140–4145, Seoul, Korea, 2001.
- [5] P. E. Gill, W. Murray, and M. A. Saunders. *User’s Guide for SNOPT 5.3: A Fortran Package for Large-Scale Nonlinear Programming*. Department of Mathematics, University of California, San Diego, 2.1 edition, 1999.
- [6] M. Hardt, J. Helton, and K. Kreutz-Delgado. Optimal Biped Walking with a Complete Dynamical Model. In *Proc. of the 38th IEEE Conf. on Decision and Control*, pages 2999–3004, Phoenix, AZ, December 1999.
- [7] Thomas R. Kane and David A. Levinson. *AUTOLEV USER’S MANUAL*. OnLine Dynamics, Inc., Sunnyvale, USA, 2001.
- [8] O. Lorch, J. Denk, J. F. Seara, M. Buss, F. Freyberger, and G. Schmidt. ViGWaM — An Emulation Environment for a Vision Guided Virtual Walking Machine. In *Proc. of the IEEE/RAS Int. Conf. on Humanoid Robots (Humanoids)*, Cambridge, Massachusetts, USA, September 2000.
- [9] K. Nagasaka, H. Inoue, and M. Inaba. Dynamic Walking Pattern Generation for a Humanoid Robot Based on Optimal Gradient Method. In *Proc. of the IEEE Int. Conf. on Systems, Man and Cybernetics*, pages 908–913, Tokyo, Japan, 1999.
- [10] C. L. Shih et al. Trajectory Synthesis and Physical Admissibility for a Biped Robot During the Single-Support Phase. In *Proc. of the IEEE Int. Conf. on Robot. and Autom.*, pages 1646–1652, Cincinnati, Ohio, 1990.
- [11] Oskar von Stryk. *User’s Guide for DIRCOL: A Direct Collocation Method for the Numerical Solution of Optimal Control Problems*. Lehrstuhl für Höhere Mathematik und Numerische Mathematik, Technische Universität, München, 2.1 edition, 1999.
- [12] M. Vukobratović, B. Borovac, D. Surla, and D. Stokić. *Biped Locomotion*, volume 7 of *Scientific Fundamentals of Robotics*. Springer-Verlag, Berlin, Germany, 1 edition, 1990.